A time-varying magnetic flux concentrator

Article *in* Journal of Physics D Applied Physics · July 2016
DOI: 10.1088/0022-3727/49/33/335003

5 authors, including:

Behailu Kibret
Monash University (Australia)
31 PUBLICATIONS **209** CITATIONS
SEE PROFILE

Malin Premaratne
Monash University (Australia)
276 PUBLICATIONS **2,923** CITATIONS
SEE PROFILE

Philip M Lewis
Monash University (Australia)
57 PUBLICATIONS **517** CITATIONS
SEE PROFILE

Richard H S Thomson
Monash University (Australia)
52 PUBLICATIONS **783** CITATIONS
SEE PROFILE

Accepted for publication in Journal of Physics D: Applied Physics

A time-varying magnetic flux concentrator

B Kibret[1], M Premaratne[1], P M Lewis[2], R Thomson[3] and P B Fitzgerald[3]

[1] Advanced Computing and Simulation Laboratory (AχL), Department of Electrical and Computer Systems Engineering, Monash University, Clayton 3800, Victoria, Australia.

[2] Department of Surgery, Faculty of Medicine, Nursing and Health Sciences, Monash University, Melbourne 3004, Victoria, Australia

[3] Monash Alfred Psychiatry Research Centre, Monash University Central Clinical School and the Alfred, Melbourne 3004, Victoria, Australia

E-mail: behailu.kibret@monash.edu

Abstract. It is known that diverse technological applications require the use of focused magnetic fields. This has driven the quest for controlling the magnetic field. Recently, the principles in transformation optics and metamaterials have allowed the realization of practical static magnetic flux concentrators. Extending such progress, here, we propose a time-varying magnetic flux concentrator cylindrical shell that uses electric conductors and ferromagnetic materials to guide magnetic flux to its center. Its performance is discussed based on finite-element simulation results. Our proposed design has potential applications in magnetic sensors, medical devices, wireless power transfer, and near-field wireless communications.

PACS numbers: 85.70.Ay, 41.20.Gz

Keywords: magnetic flux concentration, metamaterial, magnetic device

Submitted to: *J. Phys. D: Appl. Phys.*

1. Introduction

The manipulation of electromagnetic fields to paths of interest has been enabled by transformation optics (TO) [1, 2, 3]. In the technique of TO, the trajectories of fields are changed by transforming the coordinate space that allows the definition of new sets of permittivity and permeability tensors constituting the form-invariant Maxwell's equations. Normally, the permittivity and permeability obtained from applying TO requires nonhomogeneous and anisotropic materials that are not found in nature. For that reason, metamaterials are usually used to realize such effective dielectric and magnetic properties [4, 5, 6]. Examples of TO applications include the design of optical devices based on plasmonic metamaterials that exploit surface plasmons to get artificial optical properties [7]. At the other side of the spectrum, TO has also been applied to design static magnetic field cloaks [8, 9].

It has also been utilized to concentrate magnetic fields [10, 11, 12]. In [10], a nonhomogeneous and anisotropic electromagnetic field concentrating cylindrical shell was discussed. The cylindrical shell was designed based on a linear space transformation that resulted in a radial dependence in the permittivity and permeability tensors, for axial and angular field components in a cylindrical coordinate system. The radial dependency makes the cylinder difficult to realize using metamaterials. Similarly, [11] also discussed the application of TO to designing a magnetic field concentrator using homogenous and anisotropic cylindrical shell. In [11], a nonlinear space transformation was used that resulted in diagonal tensors with no radial dependence, for fields that do not have axial components. This simplified the realization of a static magnetic field concentrating cylindrical shell using ferromagnetic and superconductor metamaterial [13].

From [11], for a magnetic field concentrator cylindrical shell of axis directed towards the z-axis of a cylindrical coordinate system (ρ,ϕ,z) as shown in figure 1, and for magnetic fields with no z-components, the cylindrical shell is required to have relative permeability of

$$\mu_\rho = s, \qquad \mu_\phi = 1/s, \qquad \rho \in [R_1, R_2) \tag{1}$$

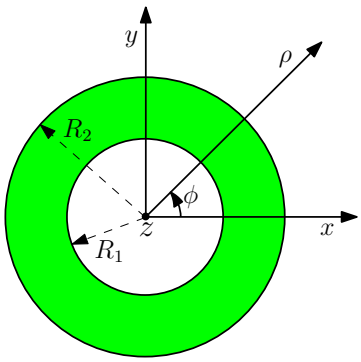

Figure 1. The cylindrical shell with inner radius R_1 and outer radius R_2.

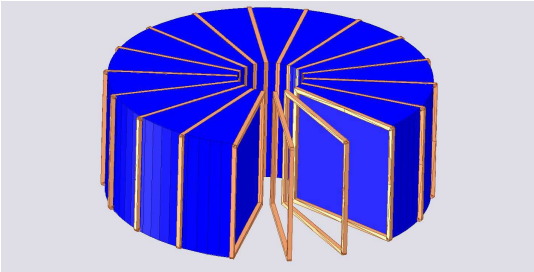

Figure 2. The time-varying magnetic flux concentrator cylindrical shell with alternately placed 18 FM wedges and 18 copper loops. The golden components are the copper loops; and the blue components are the FM wedges. For better view of the copper loops, three of the FM wedges at the front were removed in the picture.

$$\mu_\rho = 1, \qquad \mu_\phi = 1, \qquad \rho \in [0, R_1) \tag{2}$$

where R_1 is the inner radius; R_2 is the outer radius; and $s > 1$. Furthermore, considering a static magnetic field, where the magnetic and electric field are completely decoupled, there is no need to consider the permittivity tensor for the cylindrical shell. This reduces the design complexity when realizing the magnetic field concentrator. It was also shown that, assuming the cylindrical shell is placed inside a uniform static magnetic field H_o on the xy-plane, a maximum magnetic field inside the cylindrical shell, $H_i = (R_2/R_1)H_o$, can be obtained for the ideal case when $s \to \infty$. This corresponds to $\mu_\rho = \infty$ and $\mu_\phi = 0$. However, there is no natural material that has such extreme anisotropic properties; therefore, a metamaterial was used to approximately realize the cylindrical shell [13]. The cylindrical shell was realized with alternately placed ferromagnetic (FM) and superconductor (SC) wedges. The crude interpretation of the realized cylindrical shell is: the FM wedges allows the flow of the radial magnetic flux and the SC wedges impedes the angular component of the magnetic flux, with overall effect of directing the magnetic flux towards the center of the cylinder. With such an arrangement of FM and SC wedges in the cylindrical shell, an effective anisotropic permeability, which is very large in the radial direction and very small in the angular direction, can be obtained that roughly approximates the permeability expressed in (1).

In the static magnetic flux concentrator cylindrical shell [13], the SC wedges were used as diamagnetic material to oppose the angular magnetic flux. Though, they are effective and practical diamagnetic materials for static magnetic fields, their operation calls for use of cryogenic temperatures. Whilst it is difficult to find diamagnetic materials as effective as SC for static magnetic fields, electrically conductive materials are sufficiently diamagnetic in time-varying fields. Consequently, this paper focuses on the application of good conductors in place of SC in time-varying magnetic flux concentrating cylindrical shell, which is much simpler to implement into practical magnetic devices. Hence, this paper proposes a time-varying magnetic flux concentrator cylindrical shell that consists of FM wedges and copper loops in place of the SC wedges (see figure 2).

The proposed cylindrical shell makes use of the induced electric currents (eddy

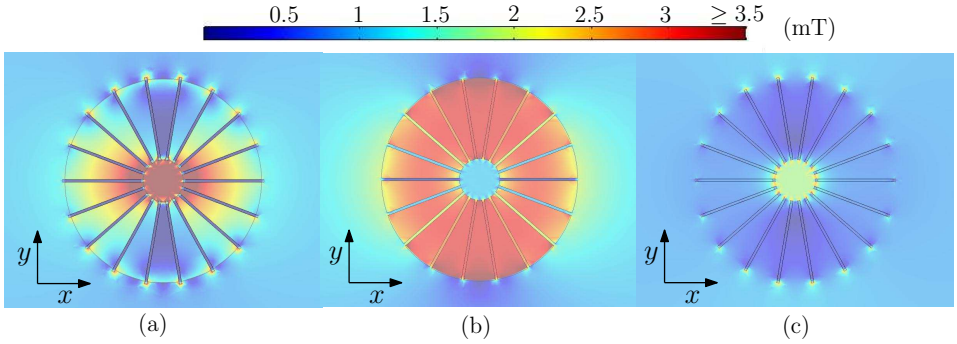

Figure 3. (a) The magnitude of the magnetic flux density distribution on a plane traversing the mid-section of the cylindrical shell when it is placed in a uniform magnetic field of 1 mT directed toward the positive x-axis at 100 kHz (b) when the cylindrical shell consists of only FM wedges (c) when the cylindrical shell consists of only copper loops

currents) in the copper loops to counteract the angular magnetic flux with similar effect to the SC wedges in the static magnetic flux concentrator cylindrical shell. For time-varying magnetic fields, the eddy currents in copper tend to get localized near the edges; thus, a loop was used instead of a wedge or a plate. Furthermore, in order to decrease the ohmic loss due to the induced eddy current, the thickness of the copper loops should be greater than the skin-depth of copper. Additionally, the FM wedges should have very low conductivity so that the eddy current induced in them is too small to counteract the radial magnetic flux. For this reason, the proposed cylindrical shell uses ferrite FM wedges, which have low conductivity.

In this paper, firstly, the performance of the proposed cylindrical shell, when it is placed inside a uniform magnetic flux, was assessed based on simulation results using COMSOL™ Multiphysics software package (COMSOL Inc., Stockholm, Sweden). From the simulation results, important characteristics of the cylindrical shell, such as, the performance dependence on frequency and dimensions of the cylinder, were investigated. However, in practical applications, the cylindrical shell would be placed near a magnetic field source; so that it might affect the source by modifying the electrical impedance. Consequently, the following part of the paper is dedicated to analyze the effects of the cylindrical shell on a magnetic field source. This was further elaborated by presenting an illustrative example by considering the scenario when the cylindrical shell is placed at the center of a single turn coil that acts as a magnetic field source. Lastly, the effect of magnetic saturation and the possibility of adding a resonant feature were touched in a separate section as additional remarks.

2. The cylindrical shell inside a uniform magnetic flux

The performance of the proposed cylindrical shell when it is placed inside a uniform magnetic flux was assessed by simulating it using the Magnetic Fields interface in the AC/DC module of COMSOL™ Multiphysics.

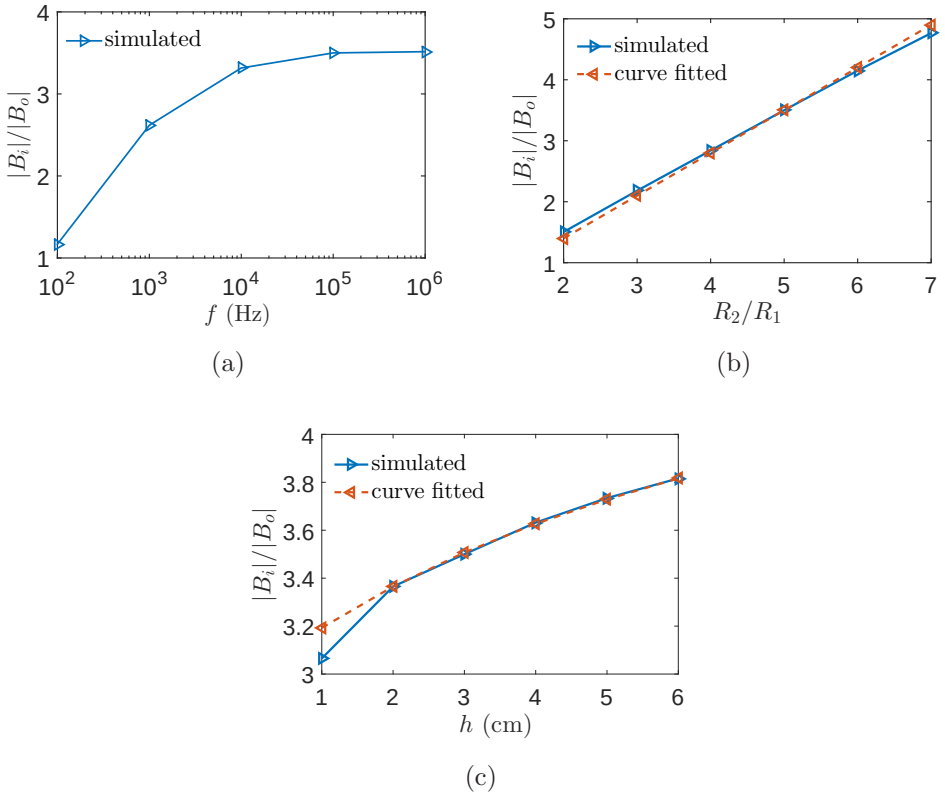

Figure 4. (a) The ratio of the magnitude of the interior magnetic flux density B_i to outer uniform magnetic flux density B_o versus the frequency of the applied magnetic field, assuming a linear response in the FM wedges. (b) The blue line shows the relationship between the $|B_i|/|B_o|$ and the R_2/R_1. (c) The relationship between the height of the cylindrical shell and the $|B_i|/|B_o|$. The red broken line in (b) and (c) shows the plot of curve fitted values.

Figure 3 shows the simulation result of the magnetic flux density distribution on a plane traversing the cylindrical shell at the mid-section when is it placed in a uniform magnetic field of flux density B_o= 1 mT at 100 kHz, which is directed toward the positive x-axis. The cylindrical shell has an inner radius R_1= 0.8 cm, outer radius R_2= 4 cm and height h= 3 cm. The FM wedges consist of ferrite with relative permeability μ_{FM}= 1500 and conductivity σ_{FM}= 10^{-6} S/m. The copper loops have a conductivity of σ_C= 5.67×10^7 S/m, relative permeability μ_c= 1 and a thickness of 1 mm. As shown in the figure, the magnetic flux density inside the cylindrical shell is 3.5 times that of the uniform magnetic field outside.

Figure 4(a) shows the relationship between the magnetic flux density inside the cylindrical shell B_i and the frequency of the applied uniform magnetic flux, which is represented by its flux density B_o. The figure shows that the flux density ratio $|B_i|/|B_o|$ increases with frequency and then saturates when most of the angular magnetic flux is effectively counteracted by the eddy currents in the copper loops. This is expected since the opposing magnetic field, which is proportional to the induced eddy currents in the copper loops, increases with frequency. For low frequencies, such as at 100

Hz, the magnitude of the induced eddy currents is very small. Figure 4(b) shows the relationship between the ratio of radii in the cylindrical shell (R_2/R_1) and the magnetic flux density ratio, with fixed values of R_2= 4 cm and h= 3 cm. When the inner radius R_1 decreases, the thickness of the cylindrical shell increases with more magnetic flux passing through the FM wedges. Moreover, figure 4(c) shows the increase in the flux density ratio $|B_i|/|B_o|$ with the increase in the height of the cylinder, where R_2= 4 cm and R_1= 0.8 cm are fixed. When the height of the cylinder increases, the area enclosed by the copper loops increases, which in turn increases the amount of induced magnetic flux that impedes the angular component of the applied magnetic flux.

From the simulation results, a relationship between the flux density ratio $|B_i|/|B_o|$ and the dimensions of the cylindrical shell (R_1, R_2, and h) was derived. For frequencies higher than 10 kHz, where $|B_i|/|B_o|$ saturates, the following relation was derived from curve fitting the simulation results,

$$\frac{|B_i|}{|B_o|} = \frac{R_2}{R_1}\left(1 - \frac{3.4311}{h + 0.4718N_w}\right) \tag{3}$$

where h is given in cm; and N_w is the number of FM components. The derived expression in (3) agrees with the theoretical prediction in [11] that the maximum possible flux density ratio $|B_i|/|B_o| = R_2/R_1$ when either $h \to \infty$ or $N_w \to \infty$. The broken line plots in figure 4(b) and figure 4(c) were obtained from (3).

3. The effect of the cylindrical shell on a magnetic field source

The simulation results in the previous section show that the proposed cylindrical shell is capable of concentrating time-varying magnetic flux. The simulation results were obtained with the assumption that the cylindrical shell was placed in a uniform magnetic flux and without considering its effect on the source of the magnetic flux. However, in practical cases, the cylindrical shell operates near a magnetic field source. Consequently, the cylindrical shell affects the impedance of the source by introducing an ohmic loss or by disturbing the reactive impedance. In particular, the cylindrical shell introduces ohmic loss from the induced eddy current inside the copper loops and the FM wedges. In addition to the ohmic loss, magnetic hysteresis in the FM wedges also contributes loss. Also, reactive impedances are introduced due to the change in self-inductance introduced by the FM wedges and the mutual inductance due to the induced eddy currents in the copper loops. Therefore, the complete characterization of the cylindrical shell, which addresses these effects, is crucial to determine the practical applicability of the proposed cylindrical shell. In this section, such effects were analyzed thoroughly and formulas were derived to describe them quantitatively.

Assuming the magnetic source is a coil with a sinusoidal current $I(t) = I_s \cos(\omega t)$, an AC resistance R_s, and a self-inductance L_s, the effect of the cylindrical shell can be represented by the equivalent electrical circuit shown in figure 5. In figure 5, M_c represents the effect of the reactive magnetic power due to the mutual inductance of the copper loops; R_o represents the effect of the ohmic loss in the copper loops; R_r represents

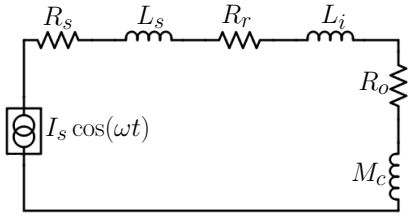

Figure 5. The equivalent circuit when the cylindrical shell is placed near a magnetic field source coil.

the effect of the power loss due to the magnetic hysteresis inside the FM wedges; and L_i represents the additional self-inductance of the coil due to the FM wedges.

3.1. The mutual inductance (M_c)

When the cylindrical shell is placed near the source coil, the electromotive force (emf) $V(t)$ induced on a single copper loop can be described as

$$V(t) = -\frac{\partial \Phi_m}{\partial t} = -\frac{\partial}{\partial t}\int_S \mathbf{B}(\mathbf{r},t)\cdot \mathrm{d}\mathbf{s} \tag{4}$$

where Φ_m is the magnetic flux passing through the area enclosed by the copper loop and $\mathbf{B}(\mathbf{r},t)$ is the magnetic flux density at the position $\mathbf{r}$; and S represents the area enclosed by the copper loop. Since the area enclosed by the copper loops is air, the magnetic flux density can be written as $\mathbf{B}(\mathbf{r},t) = \mathbf{B}(\mathbf{r})I(t) = \mathbf{B}(\mathbf{r})I_s\cos(\omega t)$, where $\mathbf{B}(\mathbf{r})$ is a position dependent vector. Thus, the emf in phasor form can be written as

$$\tilde{V} = \mathrm{i}\omega I_s \int_S \mathbf{B}(\mathbf{r})\cdot \mathrm{d}\mathbf{s}, \tag{5}$$

which can be used to calculate the mutual inductance M_n from the n^{th} copper loop as

$$M_n = \int_{S_n} \mathbf{B}(\mathbf{r})\cdot \mathrm{d}\mathbf{s}. \tag{6}$$

where S_n represents the area enclosed by the n^{th} copper loop. Since the induced eddy current on the copper loops generates a magnetic field of its own, the accurate calculation of the emf in (4) should be carried out assuming the induced current is zero, which is equivalent to assuming an infinitesimal gap on the loop that has no capacitive coupling across it.

Ignoring the proximity effect, for a cylindrical shell of inner radius R_1, outer radius R_2 and height h, the effective AC resistance R_{ac} of a single copper loop with a square cross-sectional area of thickness T can be approximately expressed as [15, 17]

$$R_{ac} = \frac{R_{dc}\xi}{2}\left[\frac{\sinh(\xi)+\sin(\xi)}{\cosh(\xi)-\cos(\xi)}\right] \tag{7}$$

where R_{dc} is the dc resistance of the copper

$$R_{dc} = \frac{2(h+R_2-R_1)}{\sigma_c T^2}; \tag{8}$$

and

$$\xi = T\sqrt{\frac{\omega\sigma_c\mu_0}{2}}. \tag{9}$$

Therefore, the induced phasor eddy current $\tilde{I}_{ed}$ on the nth copper loop can be obtained as

$$\tilde{I}_{ed} = \frac{\tilde{V}}{R_{ac} + \mathrm{i}\omega L_c} = \frac{\mathrm{i}\omega I_s M_n}{R_{ac} + \mathrm{i}\omega L_c} \tag{10}$$

where L_c is the self-inductance of the copper loop inside the cylindrical shell and it can be calculated using COMSOL$^{\mathrm{TM}}$. Consequently, the time-average reactive magnetic power P_x from all of the copper loops can obtained as

$$P_x = \frac{\mathrm{i}\omega I_s^2}{2}\frac{\omega^2 L_c}{R_{ac}^2 + \omega^2 L_c^2}\sum_{n=1}^{N} M_n^2, \tag{11}$$

which can be used to express the equivalent circuit inductance M_c as

$$M_c = \frac{\omega^2 L_c}{R_{ac}^2 + \omega^2 L_c^2}\sum_{n=1}^{N} M_n^2 \tag{12}$$

where N is the total number of copper loops.

3.2. The ohmic loss (R_o)

The ohmic loss in the copper loops is due to the electric field induced inside the copper loops that can be expressed as $\mathbf{E}(\mathbf{r}, t) = \mathbf{E}(\mathbf{r})I_s\omega\sin(\omega t)$, where $\mathbf{E}(\mathbf{r})$ is a position dependent vector. Therefore, the total time average ohmic power P_o can be expressed as [14]

$$P_o = \frac{1}{2}\sigma_c I_s^2\omega^2\int_{V_c}|\mathbf{E}(\mathbf{r})|^2\mathrm{d}v \tag{13}$$

where σ_c is the conductivity of copper; and V_c represents the volume of the copper loops. Hence, the equivalent circuit resistance R_o can be calculated as

$$R_o = 2\frac{P_o}{I_s^2} = \sigma_c\omega^2\int_{V_c}|\mathbf{E}(\mathbf{r})|^2\mathrm{d}v. \tag{14}$$

The equivalent circuit component R_o represents the amount of the average heat energy per unit time generated inside the copper loops with the relation $P_o = \frac{1}{2}R_o I_s^2$. For higher frequency and large source currents, the heat energy could be large enough to decrease the conductivity of the copper loops. It is known that the conductivity of metals is a function of the conduction electron density and the frequency of electron collision, which both depend on the temperature [20]. Generally, the conductivity decreases with the increase in temperature. The ohmic heating in the copper loops due to the time-harmonic source current can be related to the change in temperature using the simple thermodynamics relation as [20]

$$P(t) = I_s^2\sin^2(\omega t)R_o = C_h m\frac{dT}{dt} \tag{15}$$

where the phase difference with coil current was taken into account; $P(t)$ is the instantaneous value of the total ohmic loss in the copper loops; C_h is the specific heat capacity of copper; m is the mass of the copper loops; and T is the temperature. The above equation can be used to express the change in temperature ΔT as a function of time as

$$\Delta T = T - T_0 = \frac{I_s^2 R_o}{2C_h m}\left[t - \frac{\sin(2\omega t)}{2\omega}\right] \tag{16}$$

where T_0 is the initial temperature at $t = 0$. The expression in (16) implies that the temperature increases linearly with time when $t \gg 1/\omega$. Also, for $t \gg 1/\omega$, the frequency dependence of (16) is contained in the value of R_o, which implies that the temperature increases with frequency as well. Moreover, the temperature dependence of the conductivity of the copper loops can be expressed as [20]

$$\sigma = \frac{\sigma_o}{1 + \alpha \Delta T} \tag{17}$$

where σ_o is the conductivity of copper at the initial temperature and α is the resistivity temperature coefficient of copper. Equation (16) and (17) can be related to approximately calculate the change in the conductivity when the temperature changes due to the ohmic heating.

3.3. The effect of the FM wedges (R_r and L_i)

It is known that magnetic hysteresis occurs when the alignment of the magnetic domains in a material lags the applied time-varying magnetic field [18]. Considering the equivalent circuit analyzed here, the effect of magnetic hysteresis in the FM wedges can be described by assuming the magnetic flux density $\mathbf{B}(\mathbf{r}, t)$ lags the magnetic field intensity $\mathbf{H}(\mathbf{r}, t) = \mathbf{H}(\mathbf{r}) I_s \cos(\omega t)$ inside the FM wedges by a phase delay θ_p so that the magnetic flux density can be expressed as $\mathbf{B}(\mathbf{r}, t) = \mathbf{B}(\mathbf{r}) I_s \cos(\omega t - \theta_p)$, assuming a linear system. Therefore, assuming the FM wedges are isotropic and the system is operating below the point of magnetic saturation, the permeability becomes a complex value $\tilde{\mu}$ that can be defined taking the ratio of the phasors of the magnetic flux density to the magnetic field as

$$\tilde{\mu} = \frac{|\mathbf{B}(\mathbf{r})|}{|\mathbf{H}(\mathbf{r})|} e^{-\mathrm{i}\theta_p} = \mu_0(\mu' - \mathrm{i}\mu'') \tag{18}$$

where μ' and $-\mu''$ are the real and imaginary parts, respectively. When the FM material is ferrite, the complex permeability spectra can be described by two types of magnetizing process [19]: spin rotation and domain wall motion, as

$$\tilde{\mu} = \mu_0(\mu' - \mathrm{i}\mu'') = \mu_0(1 + \chi_{spin} + \chi_{dw}) \tag{19}$$

where χ_{spin} and χ_{dw} are the magnetic susceptibility of spin and domain wall motion, respectively. For the case of the cylindrical shell with FM ferrite wedges, the real part affects the self-inductance of the magnetic field source and the imaginary part is responsible for the hysteresis loss. The spin rotation can be approximated by relaxation-type frequency dispersion due to its large damping factor in ferrites. The domain wall

component is a resonant type, which is inversely proportional to the square of frequency. Accordingly, the two magnetic susceptibility expressions were described as [19]

$$\chi_{spin} = \frac{K_{spin}}{1 + i\frac{f}{f_{spin}^{res}}}, \tag{20}$$

$$\chi_{dw} = \frac{K_{dw}\left(f_{dw}^{res}\right)^2}{\left(f_{dw}^{res}\right)^2 - f^2 + i\beta f}, \tag{21}$$

where f is the frequency; K_{spin} is the static spin susceptibility; f_{spin}^{res} is the spin resonance frequency; K_{dw} is the static susceptibility of domain wall motion; f_{dw}^{res} is the domain wall resonance frequency; β is damping factor of the domain wall motion. The values of the parameters in (20) and (21) can be determined from curve fitting the measurement data of the complex permeability. In this paper, the parameters derived for sintered ferrite in [19] were used.

When the cylindrical shell is placed near the magnetic field source, the FM wedges changes the self-inductance of the source circuit and also the hysteresis introduces power loss. Thus, the total magnetic energy density in the FM wedges $U_m(\mathbf{r}, t)$, which is the sum of the stored energy density (the real part) and the heat energy density (the imaginary part), can be expressed using the complex permeability as

$$U_m(\mathbf{r}, t) = \frac{1}{2}\tilde{\mu} I(t)^2 |\mathbf{H}(\mathbf{r})|^2. \tag{22}$$

The additional work done by the source, when the cylindrical shell is placed, is equal to the total magnetic energy in the FM wedges. Thus defining a complex self-inductance $\tilde{L}$, the work done by the source can be related to the energy in the FM wedges as

$$\frac{1}{2}\tilde{L} I^2(t) = \frac{1}{2}\tilde{\mu} I^2(t) \int_{V_{fm}} |\mathbf{H}(\mathbf{r})|^2 \mathrm{d}v, \tag{23}$$

which implies that

$$\tilde{L} = \tilde{\mu} \int_{V_{fm}} |\mathbf{H}(\mathbf{r})|^2 \mathrm{d}v, \tag{24}$$

where V_{fm} represents volume of the FM wedges. Therefore, the phasor of the additional voltage generated due to the cylindrical shell can be related to the equivalent circuit components R_r and L_i as

$$\mathrm{i}\omega \tilde{L} I_s = (R_r + \mathrm{i}\omega L_i) I_s, \tag{25}$$

which can be used to obtain

$$R_r = \omega \mu_0 \mu'' \int_{V_{fm}} |\mathbf{H}(\mathbf{r})|^2 dv, \tag{26}$$

$$L_i = \mu_0 \mu' \int_{V_{fm}} |\mathbf{H}(\mathbf{r})|^2 dv, \tag{27}$$

and the relation

$$R_r = \omega \frac{\mu''}{\mu'} L_i. \tag{28}$$

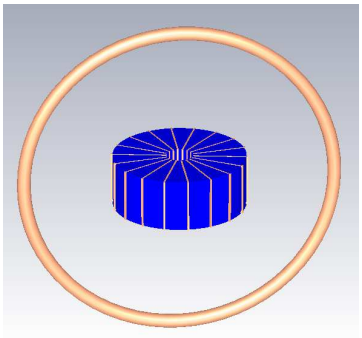

Figure 6. The cylindrical shell placed at the center of a single turn coil.

4. An illustrative example

The circuit analysis discussed in the previous section was illustrated with an example by simulating the scenario when the cylindrical shell shown in figure 2 (R_1= 0.8 cm, R_2=4 cm, h=3 cm) is placed in the center of a single turn copper coil of wire cross-sectional area of 10^{-6} m^2 and radius of 8 cm with a sinusoidal source current of amplitude I_s=1 A, as shown in figure 6. The complex permeability of the FM wedges was calculated from the parameters given in [19], assuming it is Mn-Zn ferrite. Moreover, the derived formulas in (12), (14), (26), and (27) were applied to calculate the corresponding equivalent circuit components. The vector quantities $\mathbf{E}(\mathbf{r})$, $\mathbf{B}(\mathbf{r})$ and $\mathbf{H}(\mathbf{r})$, and the related surface and volume integrals used in the derived formulas were computed using COMSOL$^{\text{TM}}$.

The calculated values of the circuit components for different frequencies are shown in table 1. When the cylindrical shell is placed at the center of the coil, the magnetic flux density at the center of the cylindrical shell increased by the ratio of $|B_i|/|B_o|$. However, this is at the expense of an ohmic loss in the copper loops $P_o = \frac{1}{2}R_o I_s^2$ and magnetic hysteresis loss in FM wedges $P_r = \frac{1}{2}R_r I_s^2$. The ohmic loss in the copper loops is much larger than the hysteresis loss in the FM wedges, since P_o is proportional to the large conductivity of copper and the square of the angular frequency ω^2. Also, the hysteresis loss increases with frequency along with μ'' that has a maximum value near 1 MHz [19]. Moreover, the additional self-inductance due to the FM wedges L_i and the mutual inductance due to the copper loops M_c decrease as frequency increases along with the real part of the complex permeability μ'. However, the value of the circuit components due to the cylindrical shell are very small compared to the circuit components of the source, which are, L_s=278.42 nH and the coil resistance R_s=7.9 mΩ approximated for the frequencies in table 1. Therefore, for this case, it can be concluded that the effect of the cylindrical shell is negligible.

Moreover, the change in temperature of the copper loops for different frequencies is shown in figure 7(a), which was calculated assuming a source current amplitude of I_s=100 A. The corresponding effect of frequency on the conductivity is shown in figure 7(b), which shows the percentage decrease in the conductivity versus time. Since the change in temperature is proportional to the square of the source current amplitude

Table 1. The equivalent circuit components

f (Hz)	μ'	μ''	$\lvert B_i\rvert/\lvert B_o\rvert$	R_r ($\mu\Omega$)	L_i (pH)	R_o (mΩ)	M_c (nH)
10^3	4721	5.176	2.855	4.863×10^{-5}	7.0823	0.03707	8.64
10^4	4720	51.75	3.3893	5.158×10^{-3}	7.4875	0.07908	4.32
10^5	4666	508.5	3.5223	0.4095	5.9811	0.3787	3.24
10^6	2784	1973	3.5296	26.13	5.8681	0.6914	2.63

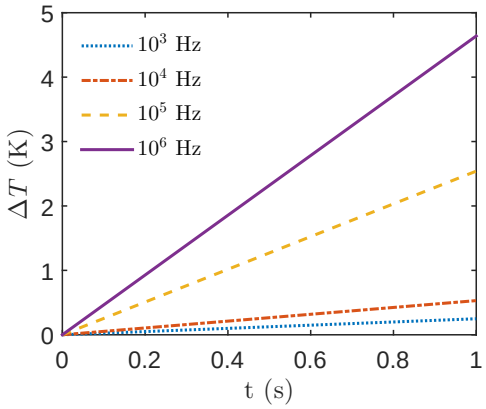

(a)

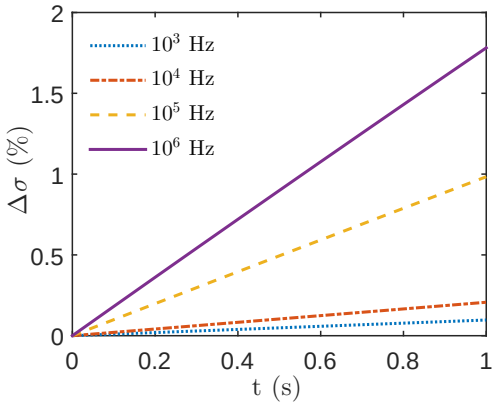

(b)

Figure 7. (a) the change in temperature versus time (b) the percentage change in the conductivity of copper versus time, for different frequencies when the amplitude of the source current I_s= 100 A.

as shown in (16), the application of the cylindrical shell in large magnetic fields might require an active cooling. Another solution to reduce temperature to a controllable level is to use source current waveforms with short duration.

The illustrative example shows that the cylindrical shell increases the magnetic flux

density at the center of the coil, which comes at the expense of the power loss in the copper loops and the FM wedges. The natural question that follows is: Is the power loss worth the increase in magnetic flux density? Other ways can be used to increase the magnetic flux, for example, increasing the source current or increasing the numbers of turns of the source coil. Consequently, we compared the power loss in the source (without the cylindrical shell) when increasing the source current or number of turns to get a 3.52 times more magnetic flux density at the center. Since the coil current and the magnetic flux density are directly proportional, the current has to be increased by 3.52 times to get an equivalent magnetic flux density at the center. Unfortunately, the power loss in the source coil is proportional to the square of the coil current; and, hence, the power loss in the coil increases by $(3.52)^2$=12.39 times. This coil power loss is 260 times more than the ohmic loss introduced by the cylindrical shell at 100 kHz, for the case of the example considered above. Also, considering the case that the number of turns is increased by 3.52, the coil power loss increases by 3.52 times since number of turns is proportional to the power loss. Also, when increasing the number of turns by 3.52, the power loss due to the source coil is 74 times more than that of the cylindrical shell at 100 kHz.

Moreover, the example represents the worst case that the cylindrical shell can affect the source, since the cylindrical shell was placed at the center of the coil where there is the largest magnetic field. When the cylindrical shell is moved to another location, the values of the additional circuit elements decrease since their value depends on the magnetic field. For example, at 100 kHz, moving the cylindrical shell a distance of 4 cm along the axis of the source coil decreased the values of the circuit element: R_r= 0.2783 $\mu\Omega$, L_i= 4.0642 pH, R_o= 0.2406 mΩ and M_c= 9.344 nH.

5. Remarks

The analysis so far was carried out assuming the FM wedges are operating below the magnetic saturation. Magnetic saturation, which is the characteristic of FM and ferrimagnetic materials, occurs when the increase in the applied magnetic field does not increase the magnetization of the material. In other words, saturation occurs when all of the magnetic domains of the material are aligned by the applied magnetic field so that the increase in the applied magnetic field does not increase the magnetic field inside the material. The saturation of ferrites occurs at relatively lower magnetic flux density ($<$ 0.5 T) when compared to other FM materials, such as, iron alloys ($<$ 2.2 T) and amorphous alloys (1.2 T) [16]. Usually, iron alloys have high conductivity, which is undesirable in the cylindrical shell due to the large eddy current in the FM wedges. The induced eddy current can be reduced by using laminated sheets of iron alloys. It was shown that when the ratio of radii (R_2/R_1) of the cylindrical shell increases, the amount of magnetic flux inside the cylindrical shell also increases. However, when R_2/R_1 increases, the inner edge of the FM wedges becomes smaller compared to the outer edge causing the build up of larger magnetic flux near the inner edge. This might cause the

FM wedges saturate at the inner edges. Therefore, this implies that in the design of the cylindrical shell, the dimensions are also determined by the amount of magnetic field used.

An interesting aspect of the proposed cylindrical shell is: it could be used to selectively concentrate magnetic field at specific frequency by utilizing the resonance of the induced eddy current on the copper loops. By introducing a capacitive element on each of the copper loops, only the magnetic field at the resonance frequency can be selectively concentrated. This suggests that the cylindrical shell can also be implemented as a filter. Assuming a capacitive element C is inserted in a small segment of the copper loop, so that the eddy current expression in (10) changes to

$$\tilde{I}_{ed} = \frac{-\omega^2 I_s C M_n}{i\omega C R_{ac} - \omega^2 L_c C + 1}, \tag{29}$$

which resonates at the resonance frequency

$$f_{res} = \frac{1}{2\pi\sqrt{L_c C}}. \tag{30}$$

A similar operation principle is implemented in split ring resonators that are usually used in microwave and terahertz frequencies [21, 22]. In split ring resonators the capacitive element is introduced using a small gap on the conductive loops.

6. Conclusion

We have proposed a time-varying magnetic flux concentrator cylindrical shell that consists of FM wedges and copper loops. Since the cylindrical shell operates near a magnetic field source, its effect on the magnetic field source was analysed and illustrated with an example. The cylindrical shell introduces an ohmic loss and a reactive impedance. However, as demonstrated with an example, these effects can become insignificant when compared to the ohmic losses introduced when the source current is increased to generate an equivalent magnetic field. The cylindrical shell has potential applications in medical devices, wireless power transfer and near-field wireless communications.

Acknowledgments

The authors would like to acknowledge Monash University Interdisciplinary Research Grants for financial support.

References

[1] J. B. Pendry, D. Schurig and D. R. Smith, *Controlling electromagnetic fields*, Science, 312(5781), 1780 (2006).

[2] U. Leonhardt, *Optical conformal mapping* Science, 312(5781), 1777 (2006).

[3] W. Zhu, I. Rukhlenko, and M. Premaratne, *Linear transformation optics for plasmonics* J. Opt. Soc. Am. B 29, 2659 (2012).

[4] D. Schurig, J. J. Mock, B. J. Justice, S. A. Cummer, J. B. Pendry, A. F. Starr and D. R. Smith, *Metamaterial electromagnetic cloak at microwave frequencies*, Science 314(5801), 977 (2006).
[5] W. Zhu, I. D. Rukhlenko, and M. Premaratne, *Graphene metamaterial for optical reflection modulation* Applied Physics Letters, 102(24), 241914 (2013).
[6] W. Zhu, F. Xiao, M. Kang, D. Sikdar, and M. Premaratne, *Tunable terahertz left-handed metamaterial based on multi-layer graphene-dielectric composite* Applied Physics Letters, 104(5), 051902 (2014).
[7] J. A. Schuller, E. S. Barnard, W. Cai, Y. C. Jun, J. S. White, and M. L. Brongersma, *Plasmonics for extreme light concentration and manipulation* Nature materials, 9(3), 193-204 (2010)
[8] B. Wood, and J. B. Pendry. *Metamaterials at zero frequency*, Journal of Physics: Condensed Matter 19(7) 076208 (2007).
[9] C. Navau, D. X. Chen, A. Sanchez, and N. Del-Valle, *Magnetic properties of a dc metamaterial consisting of parallel square superconducting thin plates*, Applied Physics Letters, 94(24), 242501 (2009).
[10] M. Rahm, D. Schurig, D. A. Roberts, S. A. Cummer, D. R. Smith, and J. B. Pendry, *Design of electromagnetic cloaks and concentrators using form-invariant coordinate transformations of Maxwells equations*, Photonics and Nanostructures-fundamentals and Applications, 6(1), 87 (2008)
[11] C. Navau, J. Prat-Camps, and A. Sanchez, *Magnetic energy harvesting and concentration at a distance by transformation optics* Physical review letters, 109(26), 263903 (2012)
[12] F. Sun, and S. He, *Transformation magneto-statics and illusions for magnets* Scientific reports, 4, 6593 (2014).
[13] J. Prat-Camps, C. Navau, and A. Sanchez, *Experimental realization of magnetic energy concentration and transmission at a distance by metamaterials* Applied Physics Letters, 105(23), 234101 (2014)
[14] M. N. Sadiku,*Elements of electromagnetics (Vol. 428)*, (New York: Oxford university press, 2001).
[15] P. L. Dowell, *Effects of eddy currents in transformer windings* Proceedings of IEE, 113(8), 1387 (1966).
[16] R. M. Bozorth, *Ferromagnetism*, (Wiley-VCH, August, 1993).
[17] J. A. Ferreira, *Improved analytical modeling of conductive losses in magnetic components* IEEE Transactions on Power Electronics,9(1), 127 (1994).
[18] G. Bertotti, *Hysteresis in magnetism: for physicists, materials scientists, and engineers*, (Academic press, 1998).
[19] T. Tsutaoka, *Frequency dispersion of complex permeability in MnZn and NiZn spinel ferrites and their composite materials* Journal of Applied Physics, 93(5), 2789 (2003)
[20] R. Serway and J. Jewett, *Physics for scientists and engineers with modern physics*, (Nelson Education, 2013).
[21] J. B. Pendry, A. J. Holden, D. J. Robbins, and W. J. Stewart, *Magnetism from conductors and enhanced nonlinear phenomena* IEEE Transactions on Microwave Theory and Techniques, 47(11), 2075 (1999).
[22] D. R. Smith, W. J. Padilla, D. C. Vier, S. C. Nemat-Nasser, and S. Schultz, *Composite medium with simultaneously negative permeability and permittivity* Physical review letters, 84(18), 4184 (2000).